Journal of Applied Pharmaceutical Research
Volume 14 Issue 2, Year of Publication 2026, Page 76 – 88
DOI: https://doi.org/10.69857/joapr.v14i2.1639

Check for updates

Research Article

JOURNAL OF APPLIED PHARMACEUTICAL RESEARCH | JOAPR
www.japtronline.com ***ISSN: 2348 – 0335***

FORMULATION, OPTIMIZATION, AND IN-VITRO DIFFUSION STUDIES OF NOVEL NIOSOMAL GEL OF MICONAZOLE NITRATE

Akash Mummoorthy, Aravind Karthikeyan, Akash Rajendran, Kaviya Suresh, Anbarasan Balu*

Article Information
Received: 15th November 2025
Revised: 20th January 2026
Accepted: 21st February 2026
Published: 15th March 2026

Keywords
Anti-fungal, Box-Behnken, Ether injection method, Niosomal gel, Transdermal drug delivery system.

ABSTRACT
Background: Miconazole Nitrate exhibits potent antifungal activity; its therapeutic potential is restricted by poor skin permeability and low aqueous solubility. To overcome these limitations, the present study aimed to develop and optimize a niosomal gel delivery system using non-ionic surfactant vesicles to enhance dermal diffusion and therapeutic efficacy. **Methodology:** The ether injection method was used to create niosomes. The results obtained from applying the Box-Behnken design (BBD) were highly instructive for the PDI, droplet size, and drug release profile. DLS was used to quantify particle size and zeta potential, and SEM was used to characterize particle morphology. The stability and compatibility were examined using DSC and FTIR. **Results and Discussion:** The optimized niosomal formulation exhibited a particle size of 180.9 ± 1.8 nm, a PDI of 0.1533 ± 0.01, and a zeta potential of –27.28 ± 0.2 mV, indicating excellent colloidal stability. The Box–Behnken model exhibited strong statistical significance (R^2 = 0.9663 for size, 0.9098 for PDI, and 0.9971 for zeta potential; $p < 0.05$). The encapsulation efficiency was 91%; the in-vitro diffusion profile followed the Hixson–Crowell model (R^2 = 0.9959), confirming a controlled-release mechanism. Compared with conventional Miconazole formulations, the optimized niosomal gel demonstrated markedly enhanced diffusion and prolonged release over 8 hours. The Carbopol-based gel exhibited suitable viscosity (3250 cP), spreadability, and pH (5.5 ± 0.1), ensuring dermal compatibility. **Conclusion:** The niosomal gel displayed characteristics that improved its drug loading, stability, and sustained-release properties. These modifications indicate its potential as a transdermal drug delivery system and improved antifungal activity.

INTRODUCTION

Miconazole nitrate is an antifungal azole medication [1]. It is effective against most pathogenic fungi, including dermatophyte species [2], Candida [3], and Aspergillus [4]. The medication inhibits the action of the enzyme 14α-lanosterol demethylase [5], which is highly important in ergosterol biosynthesis. It induces the formation of additional pores in the fungal cell membrane,

*Department of Pharmaceutics, Sri Ramachandra Faculty of Pharmacy, Sri Ramachandra Institute of Higher Education and Research, Chennai, India.

***For Correspondence:** **anbarasan.b@sriramachandra.edu.in**

eventually leading to the fungus's death. It is used primarily topically as creams, gels, powders, and suppositories, and forms a critical component of the management of skin infections, vaginal candidiasis, and oral candidiasis [6,7]. Miconazole nitrate is still a crucial component of modern antifungal therapy due to its excellent safety profile and low risk of resistance [8] [9]. Surfactant-formulated colloidal drug delivery carriers, including niosomes [10], are powerful delivery systems used for the improvement of transdermal drug delivery [11] for controlled release of the drug, and for maximum systemic absorption [12]. They are highly appreciated for their non-toxicity, cost-effectiveness, and greater stability over longer periods, making them an emerging strategy in pharmaceutical formulations [13]. Niosome, patented in 1975 for dermal use [14]. They have since contributed to various commercial products, including Lancome Niosome Plus, an anti-aging product. Also, proniosomal carrier systems [15,16], e.g., curcumin mixed with Span 80 and cholesterol via the ether injection method, have been formulated to enable more effective drug penetration through the skin [17]. Among non-ionic surfactants, Span 20 (sorbitan monolaurate) and Span 80 (sorbitan monooleate) are widely utilized for niosomal preparation. In the present study, Span 20 was selected owing to its higher hydrophilic–lipophilic balance (HLB - 8.6) and a shorter alkyl chain, which favour the formation of smaller, more uniform vesicles with improved entrapment efficiency and stability. In contrast, Span 80 (HLB - 4.3) tends to form larger vesicles with less consistent dispersion due to its greater lipophilicity. Therefore, Span 20 was considered more suitable for achieving a stable, homogeneous niosomal system optimized for dermal delivery of Miconazole Nitrate. Therefore, miconazole nitrate-loaded niosomes were developed using the ether injection method for the treatment of fungal skin infections. This method can be an effective alternative to traditional drug carriers, maximizing the therapeutic effect and reducing exposure to the whole body. The effect of changing the cholesterol-to-surfactant (w/w) ratio was also investigated to improve niosome formulation [18], thereby allowing the drug to penetrate the skin and reach the site of action effectively [19]. Niosome gels, which provide improved drug solubilization, enhanced skin penetration, and controlled release, are a recent development in transdermal drug delivery systems [20,21]. Bio-compatible polymeric nanoparticles inserted into a hydrogel matrix form a structured network that regulates drug diffusion and penetration through the stratum corneum using nanoparticle-driven systems. By facilitating site-specific distribution and increasing bioavailability, the nanoscale carriers reduce systemic absorption along with related toxicity. In addition, the hydrogel's viscoelastic qualities enhance sustained pharmacological activity by extending the drug's residence time at the application site. A highly successful method for localized and regulated therapeutic administration, this synergistic technique improves patient compliance and increases the effectiveness of transdermal drug delivery [22].

MATERIALS AND METHOD

Miconazole Nitrate, cholesterol, chloroform, carbon tetrachloride, sodium hydroxide, potassium dihydrogen orthophosphate, and diethyl ether were purchased from Sigma-Aldrich.

Fabrication of niosomes

Niosomes loaded with Miconazole Nitrate were prepared using a modified ether injection method [12]. Cholesterol and non-ionic surfactants (Span 20 & Span 80) were accurately weighed & dissolved in a mixture of diethyl ether & carbinol in a clean, dry flask. Miconazole Nitrate was then incorporated into the lipid phase to ensure uniform dispersion (Table 1). The resulting organic solution was gradually injected through a 22-gauge needle at a controlled rate of 1 mL/min into 25 mL of phosphate buffer (pH 7.4) maintained at 60–65 °C under constant magnetic stirring. The temperature differential between the lipid solution and aqueous phase promoted rapid ether evaporation, leading to the spontaneous formation of stable nanosized niosomal vesicles.

Table 1: The Formulation Composition of Niosome Samples with Various Ratios and Surfactants.

S. No	Code	Surfactant	Drug: surfactant: cholesterol	Weight taken (mg)		
				Drug	Surfactant	Cholesterol
1	NF-1	S20	1:1:1	50	50	50
2	NF-2		1:1.5:1	50	75	50
3	NF-3		1:2:1	50	100	50
4	NF-4	S80	1:1:1	50	50	50
5	NF-5		1:1.5:1	50	75	50
6	NF-6		1:2:1	50	100	50

Optimization process

A Box-Behnken design comprising 13 experimental runs was employed to systematically investigate the influences of three independent variables (Table 2) on three response variables: % Drug Release, Droplet Size, and Polydispersity Index (PDI). This experimental design was adopted to facilitate the development of an optimal niosome formulation by optimization via a Box-Behnken Design strategy using Design Expert® software to plan & analyze experiments [23].

The model-derived equation based on the experimental data showed a good fit, as demonstrated by high R^2 values (all $p < 0.05$), indicating significance. The importance of the terms in the models was determined using P and F values [24]. Each experimental run generated by the Box–Behnken design was performed in triplicate (n = 3), and the mean ± SD was reported. deviation was used for all response variables to ensure the model's statistical reliability.

Table 2: Adopted Box – Behnken Design for the study

S. No	Numeric	Independent Variables	Units	Low	High
1.	A	Surfactant	Mg	50	100
2.	B	Volume of hydration	Ml	7.5	15
3.	C	Sonication	Min	2.5	5

Formulation of Miconazole Nitrate-Loaded Niosomal Gel

The gel base was formed by gradually sprinkling a known quantity of Carbopol 934 into distilled water under gentle stirring with a glass rod to ensure uniform dispersion. The optimized niosomal dispersion was then incorporated into the gel base with continuous mixing until a smooth, homogeneous gel was obtained. The pH was adjusted by adding triethanolamine (TEA) dropwise until the desired value was reached (Table 3). The final formulation was stored at 4 °C for at least 24 hrs before performing rheological evaluations.

Table 3: Formulation of Niosomal gel

Ingredients	Quantity
Niosomal dispersion	7.5ml
Carbopol 934	0.5gms
TEA	0.5gms
Distilled water	42.5ml to Q. S.

Vesicle size and Vesicle size Distribution

PDI and mean vesicle size were measured using DLS with a Malvern Zeta-sizer at a room temperature of 25 °C. Before analysis, the prepared sample was carefully inserted into a clean plastic cuvette. The formulations were appropriately diluted with phosphate buffer (pH 7.4) to achieve the best particle size and distribution. In particular, 10 µL of the diluted dispersion was poured into the cuvette for measurement after being properly mixed in a 2 mL standard volumetric flask. During size distribution analysis, this process reduced various scattering effects and guaranteed an ideal scattering intensity.

Zeta Potential (ZP)

To assess the surface charge properties of the vesicular system, zeta potential analysis was carried out concurrently at 25 °C. As an essential variable controlling the electrostatic repulsion between particles, the zeta potential sheds light on the formulation's colloidal stability and propensity for aggregation. To provide precise electrophoretic mobility measurements and to keep conductivity within the instrument's operating range, samples were suitably diluted. The physical stability profile of the developed formulation was then interpreted using the obtained zeta potential values.

Morphological Investigation of Niosomes

In characterizing niosomal vesicles, surface shape is a crucial characteristic. SEM was used to analyze the vesicular morphology, including roundness, surface smoothness & the possibility of aggregation formation. The samples were carefully placed on sterile aluminium stubs that had been pre-treated with ethanol or isopropyl alcohol (IPA) to remove impurities before imaging. To improve conductivity & avoid charging under the electron beam, a thin layer of gold was sputter-coated onto the mounted samples. After the sample was prepared, the stubs were placed in a High-Resolution SEM (HRSEM) chamber & vesicle images were acquired at appropriate magnifications to evaluate the size distribution and morphological characteristics of the vesicles.

Calculation of entrapment efficiency

Centrifugation was used to determine the miconazole nitrate's encapsulation efficiency within the niosomal vesicles. In short, the unentrapped substance was separated by cold centrifugation of 1 mL of the produced formulation at 4000 rpm for 1 hour at 4 °C. After careful extraction, the resulting supernatant was diluted with phosphate buffer (pH 7.4). A UV-visible spectrophotometer was then used to measure the absorbance of the clear solution at 231 nm. The following equation was used to compute the encapsulation efficiency (EE):

$$\boldsymbol{EE}\ (\%) = \frac{\boldsymbol{Total\ Drug\ -\ Free\ drug}}{\boldsymbol{Total\ drug}} \times \mathbf{100}$$

In-Vitro Diffusion Analysis

The niosomal formulations were analysed using a Franz diffusion cell, in which the optimized niosomal formulation was placed in the donor compartment, separated from the receptor phase by a cellophane dialysis membrane. The membrane was pre-soaked overnight in phosphate buffer (pH 7.4) to ensure proper hydration and uniform permeability. Membrane suitability was validated by confirming negligible drug adsorption and consistent diffusion of a standard Miconazole Nitrate solution. The receptor compartment contained phosphate buffer (pH 7.4) maintained under sink conditions, ensuring that the dissolution medium possessed at least a tenfold greater solubility capacity than the total drug diffused at any time point. The system was maintained at room temperature (37 ± 0.5 °C) with continuous stirring to ensure uniform distribution. Samples were withdrawn at predetermined intervals, filtered & analysed spectrophoto- metrically at 272 nm using a validated UV–visible method. All experiments were conducted in triplicate (n = 3), and results were expressed as mean ± SD, with %RSD values maintained below 2%, confirming the reproducibility of drug quantification.

pH Measurement

pH of gel preparations was measured using a digital pH meter to ensure stability and skin compatibility. 1 g of niosomal gel was suspended in 100 mL of distilled water per determination and equilibrated for 2 hours. pH was then recorded, and every formulation was tested in triplicate for accuracy and reproducibility.

Viscosity Analysis

The viscosity of the niosomal gel was measured using a Brookfield Viscometer to evaluate its rheological behaviour and spreadability. A precisely measured weight (25 ± 0.001 g) was used for testing on spindle 64 at a shear rate of 12 rpm. A measurement was obtained at room temperature to guarantee data repeatability and reproducibility.

Spreadability Study

An accurate quantity of niosomal gel was placed in the middle of a slide on a level surface. Another glass slide was carefully placed on top to ensure even contact. The initial edge of the gel was indicated on the bottom slide before a recognized weight was placed on the top slide, where it remained under tension for five minutes. After five minutes, the weight was lifted, and the spread diameter at the end was taken with a ruler or caliper. The spreadability (S) of the niosomal gel was determined with a standard formula to determine how easily it spreads and how well it is applied. The calculation was taken from the formula,

$$S = \frac{M \times L}{T}$$

*S - Spreadability (g*cm/s), M - Applied weight (g), L - Diameter of the spread gel (cm), T - Spreading time of the gel (s), which was generally taken over 300 seconds (5 minutes)*

RESULTS AND DISCUSSION

Preliminary Studies of Niosome Formulation

The preliminary studies on the preparation of the niosome formulation used span 20 and span 80 by the ether injection method. Different surfactant ratios (span 20 and span 80) were investigated, followed by the evaluation of the size, zeta potential, and polydispersity index (PDI) for each formulation. Span 20-based formulations showed better efficacy than span 80-based ones. Based on these results, the formulation with a span of 20 was selected for further optimization and characterization studies.

Earlier investigations of antifungal niosomal formulations, including works that employed the conventional thin-film hydration method (e.g., Mishra & Gupta 2022) [25] and those by Shah et al. 2023 [26] Using factorial designs, vesicle characteristics and release kinetics were typically evaluated, but formulation variables were not systematically correlated with performance outcomes through statistical optimization.

In contrast, the present study adopts a rigorous response-surface methodology (Box–Behnken design) to quantitatively optimise critical factors, yielding nanosized, uniform vesicles (~181 nm) with 91% entrapment efficiency and validated predictive models ($p < 0.05$, high R^2). This statistically-driven approach closes the methodological gap evident in earlier descriptive antifungal niosomal gel research. The enhancement in vesicle stability with increasing Span 20 concentration can be explained thermodynamically. Higher surfactant content lowers the interfacial free energy (ΔG) at the aqueous–lipid interface, promoting spontaneous and uniform vesicle formation. The higher HLB (8.6) and short alkyl chain of Span 20 favour tight molecular packing, reducing system entropy and preventing vesicle coalescence. Beyond the optimum level, however, excess surfactant increases viscosity and micellar interactions, which may compromise bilayer stability (Figure 1-3).

Optimization of Niosome

A Box–Behnken Design (BBD), a response surface methodology (RSM) that performs well for multifactorial studies, was used to systematically optimize Miconazole Nitrate-loaded niosomal formulations. This approach allowed the finding of quantitative relationships between independent formulation variables and the resulting physicochemical features of the vesicles. Effect of Formulation Variables on Vesicle Characteristics: The influence of formulation parameters on particle size, polydispersity index (PDI), and zeta potential was evaluated through ANOVA, and the outcomes are presented in Tables 4-6. The overall findings confirmed that the developed models were statistically significant, validating their suitability for explaining the variation in the measured responses.

Table 4: Optimization of Miconazole Nitrate-Loaded Niosomes Using Box–Behnken Design

Std Run	A: Surfactant (mg)	B: Volume of hydration (ml)	C: Sonication (min)	Particle size (nm)	PDI	Zeta potential (mV)
1	50	7.5	3.75	218.1 ± 2.5	0.315 ± 0.01	-21.85 ± 0.3
2	100	7.5	3.75	377.5 ± 4.1	0.5447 ± 0.02	-32.44 ± 0.5
3	**50**	**15**	**3.75**	**180.9 ± 1.8**	**0.1533 ± 0.01**	**-27.28 ± 0.2**
4	100	15	3.75	373 ± 3.5	0.5215 ± 0.02	-16.35 ± 0.4
5	50	11.25	2.5	210.1 ± 2.2	0.253 ± 0.01	-30.53 ± 0.3
6	100	11.25	2.5	345 ± 3.0	0.2888 ± 0.02	-26.84 ± 0.3
7	50	11.25	5	207 ± 2.0	0.3904 ± 0.02	-31.12 ± 0.5
8	100	11.25	5	376.2 ± 4.2	0.5431 ± 0.02	-22.86 ± 0.4
9	75	7.5	2.5	315.7 ± 3.5	0.5372 ± 0.02	-30.31 ± 0.5
10	75	15	2.5	270.2 ± 2.8	0.2731 ± 0.02	-30.31 ± 0.4
11	75	7.5	5	316.3 ± 3.6	0.4679 ± 0.02	-3.77 ± 0.3
12	75	15	5	275 ± 2.9	0.4562 ± 0.02	-21.68 ± 0.3
13	75	11.25	3.75	314 ± 3.0	0.3773 ± 0.02	-21.02 ± 0.3

All experiments were performed in triplicate (n = 3). Data are presented as mean ± SD, and standard error of the mean (SEM) was calculated.

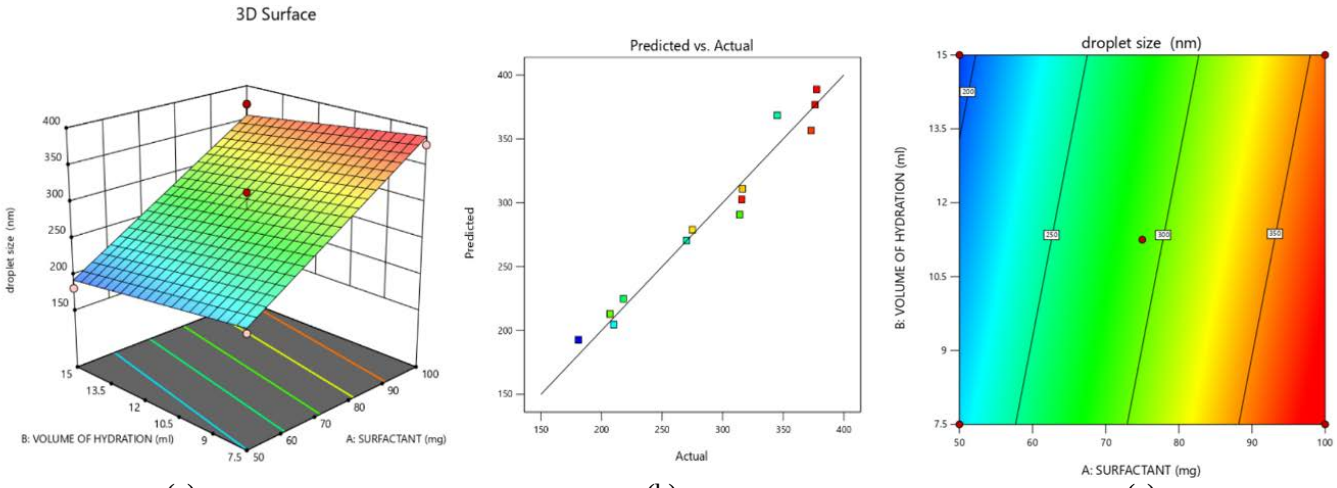

(a) (b) (c)

Figure 1: Particle size (a) 3D MODEL, (b) predicted vs Actual, (c) Contour Plot

Table 5 (a) Response 1: Particle Size

Source	Sum of Squares	df	Mean Square	F-value	p-value	
Model	55930.73	3	18643.58	85.85	< 0.0001	significant
A-Surfactant (Span 20)	53726.42	1	53726.42	247.41	< 0.0001	
B-Volume of hydration	2064.03	1	2064.03	9.50	0.0131	
C-Sonication	140.28	1	140.28	0.6460	0.4423	
Residual	1954.38	9	217.15			
Cor Total	57885.11	12				

For particle size (Figure 1) (Table 5a), the model showed a highly significant effect (F = 85.85, p < 0.0001). Among the variables, surfactant concentration (Span 20) emerged as the most influential factor (p < 0.0001), contributing predominantly to the reduction in vesicle size. This could be attributed to surfactant molecules' ability to lower interfacial tension and facilitate the formation of smaller, more stable vesicles.

The volume of hydration also exhibited a significant but comparatively weaker effect (p = 0.0131), possibly due to its role in modulating the dispersion environment and vesicle swelling. Conversely, sonication time did not significantly affect particle size (p = 0.4423), suggesting that beyond a certain threshold, additional energy input may not substantially reduce particle size.

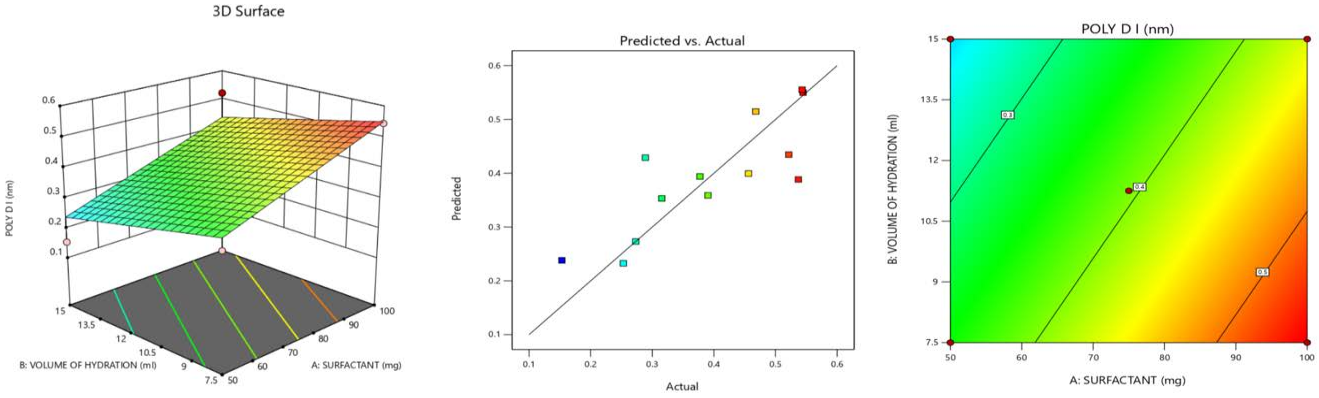

(a) (b) (c)

Figure 2: PDI (a) 3D MODEL, (b) predicted vs Actual, (c) Contour Plot

Table 5 (b) Response 2: PDI

Source	Sum of Squares	df	Mean Square	F-value	p-value	
Model	0.1357	3	0.0452	6.24	0.0140	significant
A-Surfactant (Span 20)	0.0772	1	0.0772	10.65	0.0098	
B-Volume of hydration	0.0266	1	0.0266	3.67	0.0878	
C-Sonication	0.0319	1	0.0319	4.40	0.0652	
Residual	0.0653	9	0.0073			
Cor Total	0.2010	12				

With respect to PDI (Figure 2) (Table 5b), the model was again significant (F = 6.24, p = 0.0140), indicating that the studied variables influenced vesicle homogeneity. Surfactant conc. had the strongest effect (p = 0.0098), reinforcing its role in improving size uniformity by stabilizing vesicle surfaces and preventing aggregation. Both hydration volume (p = 0.0878) and sonication time (p = 0.0652) showed near-significant trends, suggesting that they may contribute modestly to distribution uniformity but were not statistically conclusive within the studied ranges. Overall, the findings highlight surfactant optimization as the critical factor for achieving lower PDI values.

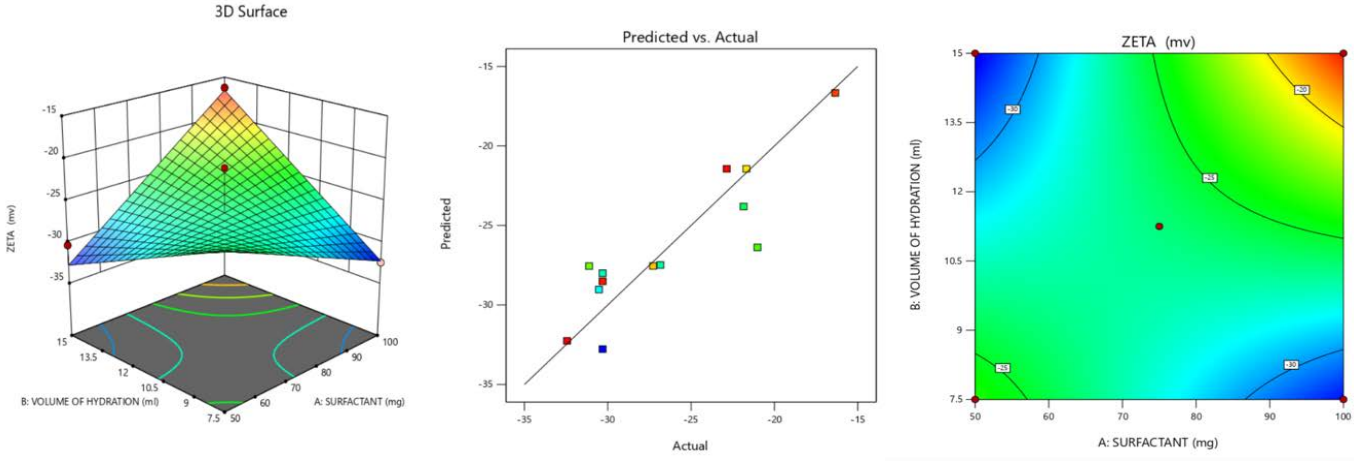

(a) (b) (c)

Figure 3: Zeta Potential (a) 3D MODEL, (b) predicted vs Actual, (c) Contour Plot

Table 5 (c) Response 3: Zeta Potential

Transform: Inverse

Source	Sum of Squares	df	Mean Square	F-value	p-value	
Model	0.0009	9	0.0001	13.62	0.0273	significant
A-Surfactant (Span 20)	0.0001	1	0.0001	14.59	0.0316	
B-Volume of hydration	0.0001	1	0.0001	11.55	0.0425	
C-Sonication	0.0001	1	0.0001	8.42	0.0624	
AB	0.0005	1	0.0005	62.34	0.0042	
AC	0.0000	1	0.0000	1.66	0.2884	
BC	0.0000	1	0.0000	2.94	0.1849	
A^2	0.0000	1	0.0000	2.46	0.2148	
B^2	0.0000	1	0.0000	1.38	0.3248	
C^2	0.0002	1	0.0002	20.34	0.0204	
Residual	0.0000	3	7.624E-06			
Cor Total	0.0010	12				

For zeta potential (Figure 3) (Table 5c), the transformed model was significant (F = 13.62, p = 0.0273), reflecting the adequacy of the selected variables in predicting colloidal stability. Surfactant concentration (p = 0.0316) and hydration volume (p = 0.0425) both exhibited significant effects, indicating their combined role in imparting electrostatic stability to the vesicles. Although sonication showed only a marginal effect (p = 0.0624), the interaction between surfactant and hydration volume (AB) was highly significant (p = 0.0042), suggesting a synergistic impact on surface charge distribution. Interestingly, a quadratic effect of sonication (C^2) was also significant (p = 0.0204), implying that beyond a certain level, sonication energy may alter the vesicle surface charge and thus influence stability. The fundamental molecular effects of formulation factors on vesicle formation, stability, and drug-release behaviour were clarified by interaction plots and 3D surface response studies. Due to increased surfactant volume and decreased interfacial free energy (ΔG) at the aqueous–lipid interface, an increase in surfactant concentration (Span 20) significantly reduced vesicle size and PDI, encouraging the production of homogeneous, thermodynamically stable bilayers. However, partial vesicle coalescence and size enlargement were caused by enhanced micellar interactions and medium viscosity beyond the critical surfactant threshold. The volume of hydration exhibited a dual influence: adequate hydration promoted complete lamellar swelling and efficient drug entrapment, whereas excessive aqueous volume caused vesicle dilution and partial drug diffusion into the medium, thereby lowering encapsulation efficiency. Sonication time significantly affected vesicular morphology and bilayer integrity: controlled sonication facilitated uniform vesicle breakdown and stabilization by reducing lamellar stacking, whereas prolonged sonication induced structural disruption and potential drug leakage due to localized thermal stress. When combined, these findings highlight that the most important element affecting all three responses is surfactant concentration. While sonication has a limited direct effect, it contributes through quadratic and interaction terms. Hydration volume plays a supportive but important role, especially in altering zeta potential and particle size. Thus, the interaction of these variables provides a foundation for optimizing formulation parameters to produce stable vesicles with desired physicochemical characteristics.

Table 6: Summary of the model results for regression analysis of responses R1–R3

Model Type	Response	R^2	Adjusted R^2	Predicted R^2	SD	%CV
Linear	Particle Size (R1)	0.9663	0.9548	0.9231	14.74	6.91
Linear	PDI (R2)	0.9098	0.8765	0.8212	0.0854	9.41
Quadratic	Zeta Potential (R3)	0.9971	0.9814	0.9445	0.0027	3.26

Validation of the Statistical Model

Validation of the statistical model was confirmed by comparing predicted and experimental values for the optimized formulation F1 (Table 6). For particle size, the experimental value (180.9 ± 1.8 nm) was in close agreement with the predicted value (182.3 nm), with a relative error of only 0.77%, demonstrating high model precision. Similarly, for PDI, the experimental value (0.1533 ± 0.01) was nearly identical to the predicted value (0.1498), with a relative error of 2.28%. For zeta potential, the experimental value (-27.28 ± 0.2 mV) closely matched the

predicted value (-26.95 mV), showing a relative error of 1.21%. These minimal errors highlight the robustness and reliability of the applied box-Behnken model. The results confirm that the developed regression models accurately predict the effects of formulation variables on particle size, PDI, and zeta potential, thereby ensuring reproducibility of the optimized niosomal formulation.

Solubility studies

Miconazole Nitrate solubility profile indicates poor water solubility and high carbinol solubility. Hence, carbinol was used as a calibrating curve medium.

Standard Calibration

In preparing solutions, 10 mg of miconazole nitrate was accurately weighed and transferred to a 10 mL volumetric flask. The linear regression equation Y = 0.1999x + 0.1827, for which the coefficient of determination (R^2) was 0.9973 at 231nm. This equation describes the linear relationship between the concentration (x) of Miconazole nitrate and the corresponding absorbance values (Y) at the specified wavelength. Such a high R^2 value indicates that approximately 99.73% of the variance in the absorbance value. Thus, the calibration curve (Figure 4) is accurate and highly precise for the determination of Miconazole Nitrate concentration in samples based on absorbance at 231 nm.

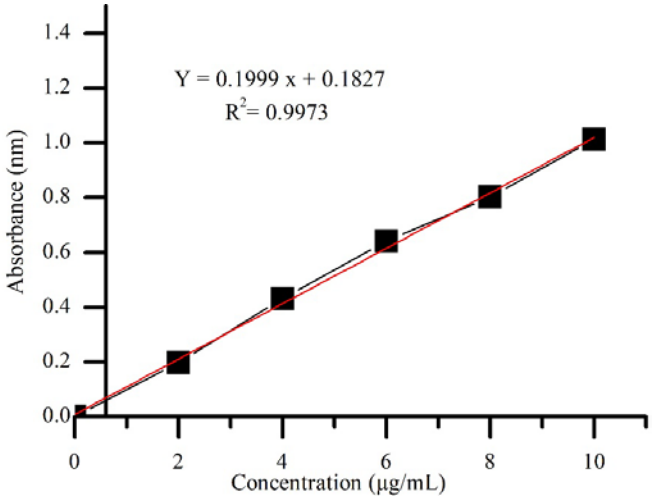

Figure 4: Linearity curve of miconazole nitrate

Particle size, PDI, Zeta potential

The optimised formulation's particle size, PDI, and Zeta potential were analyzed using Malvern Zeta Sizer. The optimized niosome size is 180.9 ± 1.8 nm. The Polydispersity Index (PDI) of the optimized niosome is 0.1533 ± 0.01. The Zeta Potential of the optimized nanoparticles is found to be -27.28 ± 0.2. Thus, the optimized formulation F1 was developed based on the overlay plot results in particle size within its ranges.

Fourier transform infrared (FTIR) spectroscopy

FTIR spectroscopy of the drug, span, cholesterol, and the optimized formulation was investigated to determine their chemical interactions and functional group behavior. Peaks were not overlapped between the drug and excipients, such as cholesterol. The peak wave number associated with the functional group is given below for drug A (Miconazole nitrate), B (Span 20), C (Cholesterol), and D (Optimal Formulation) (Figure 5).

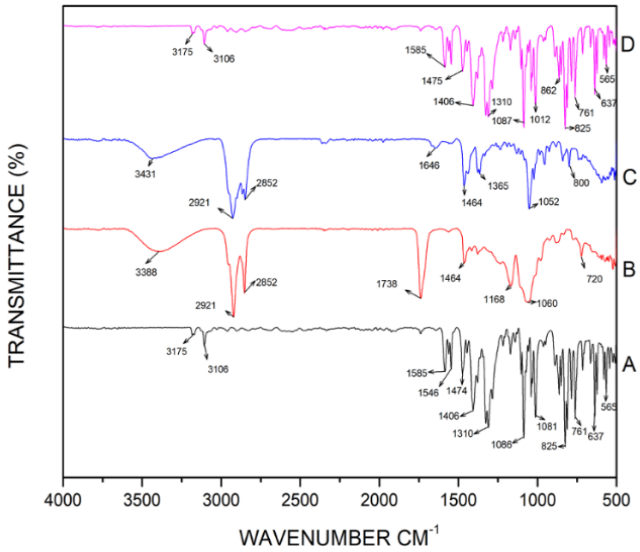

Figure 5: FTIR graph

The FTIR spectra provided useful information about the functional groups present in the materials. Miconazole Nitrate showed characteristic peaks at 3175 cm^{-1} (N-H), 1585 cm^{-1} (C=C), 1474 cm^{-1} (C-H), 1310 cm^{-1} (N-O), 1081 cm^{-1} (C-O), and 761 cm^{-1} (C-Cl). Span 20 showed C-H stretching vibrations at 2921 cm^{-1} and 2852 cm^{-1}, and C-H bending at 1464 cm^{-1} and 1374 cm^{-1}, and other peaks referring to C=O, C-O, C-N, and C-H groups. Spectra of cholesterol showed C-H stretching at 2921 cm^{-1} and 2852 cm^{-1}, C=C stretching at 1646 cm^{-1}, and peaks showing S=O and C-Cl groups. FTIR characterization of the optimized formulation mixture preserved the major functional groups of Miconazole Nitrate and Cholesterol, such as N-H, C=C, C-H, N-O, and C-Cl, which confirms their successful integration. These spectral observations confirm the chemical compatibility between Miconazole Nitrate and excipients. The preservation of key functional groups without major peak shifts indicates that the drug is physically encapsulated within the bilayer, maintaining its structural integrity and ensuring formulation stability.

Differential Scanning Calorimeter (DSC)

The thermal profile of pure Miconazole Nitrate exhibits a sharp melting endotherm at 185 °C, whereas the optimized niosomal formulation shows an altered thermal event at 159 °C, accompanied by attenuation of the original melting feature. This change in thermal behaviour suggests a modification of the drug's solid state on incorporation into the niosomal matrix. Possible explanations include partial reduction in crystallinity (partial amorphization), formation of a different crystalline habit/polymorph, or a drug–excipient physical association that modifies the thermal transitions. Taken together with the unchanged FTIR fingerprint, these data most consistently indicate physical dispersion/partial disordering of Miconazole within the bilayer (leading to improved apparent solubility and altered thermal response) rather than covalent degradation. We therefore conclude that the drug is physically incorporated, with altered solid-state characteristics likely to enhance dissolution.

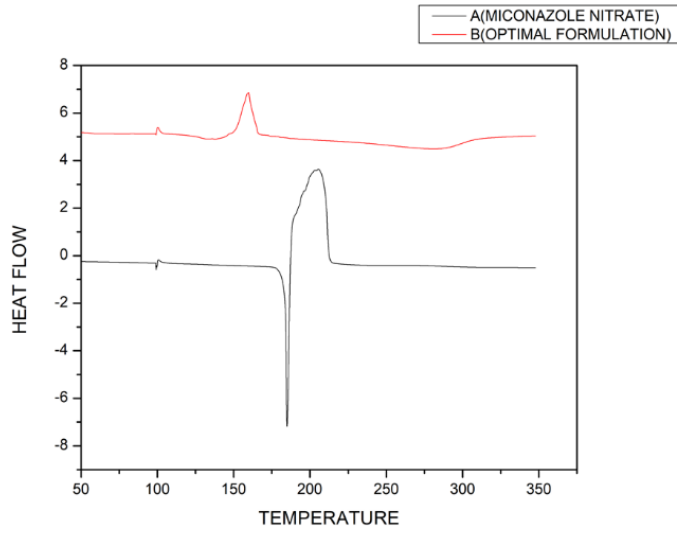

Figure 6: Thermal Peak Graph

Scanning electron microscopy (SEM)

The apparent discrepancy between the vesicle sizes obtained from DLS (180.9±1.8nm) & SEM (500nm) arises from the fundamental difference in measurement conditions. DLS evaluates the hydrodynamic diameter of vesicles in their fully hydrated & dispersed state, which includes the hydration layer surrounding the particles. In contrast, SEM imaging is performed under vacuum after solvent evaporation, where dehydration can cause partial vesicle collapse or fusion, leading to an apparent increase in observed particle size. Such variations between dry-state and hydrated-state analyses are well-documented in vesicular systems and do not indicate actual instability of the formulation.

The optimized miconazole nitrate formulation exhibited significant morphological characteristics (F1). Successful niosome formation was confirmed by the SEM photomicrographs, which indicated a distribution of spherical particles with a primary particle size of 500 nm. Good formulation stability was shown by the particles' smooth surface and lack of aggregation (Figure 7). This uniform distribution of nanoscale particle sizes has the potential to improve drug solubility and bioavailability. Overall, the SEM analysis confirmed that the F1 formulation has the qualities needed for efficient drug delivery.

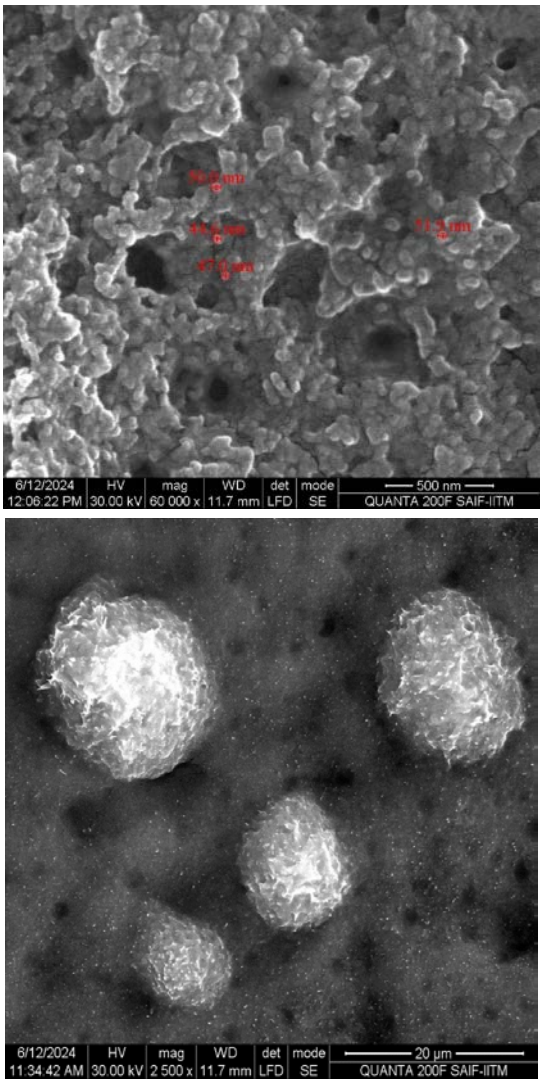

Figure 7: The SEM photomicrographs

Entrapment Efficiency

The study divides entrapment efficiency into three grades: low (F3), moderate (F2), and high (F1). The drug is effectively entrapped by formulations F1 (91%), F6 (88%), and F13 (86%), which show significant entrapment efficiencies. The efficiency of formulas F2, F5, F8, and F12 is moderate. Low efficiency in

formulations F9, F11, and F3 indicates less successful trapping and less effective treatment.

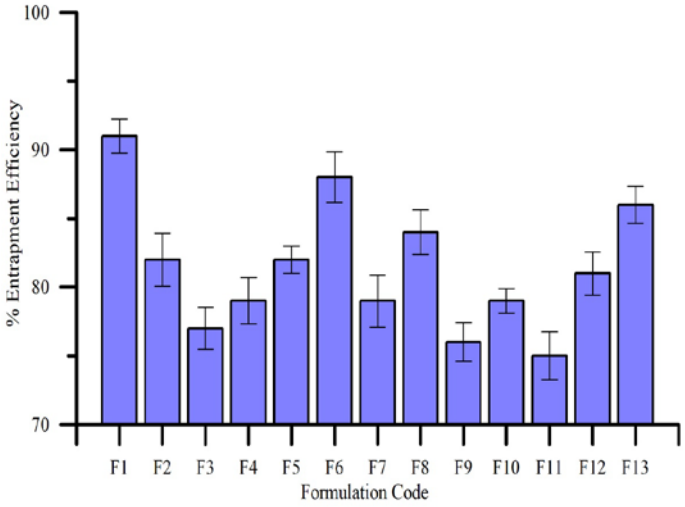

Figure 8: Comparison of Entrapment Efficiencies

Based on the evaluation results for various niosome formulations, F1 was found to yield the optimal results and was suitable for further processing (Figure 8). Formulation F1 was used to prepare the gel.

In-vitro Dissolution

In-vitro diffusion studies of the Miconazole Nitrate-loaded niosomal formulations (F1–F13) were carried out using a Franz diffusion cell system at 37 ± 0.5 °C for 8 h. Among the evaluated batches, formulation F1 exhibited the most favorable diffusion behavior, achieving a cumulative drug release of 75.0 ± 2.2% at 8 h, which was significantly higher than that observed for the conventional Miconazole gel (approximately 60% at 8 h). The diffusion rate constant (*k*) derived from the Hixson–Crowell kinetic model was 0.123 h^{-1} (R^2 = *0.9959*), confirming an erosion-controlled release mechanism. The enhanced diffusion from the optimized formulation can be attributed to its nanosized vesicles (~180 nm), narrow distribution (PDI = 0.1533), and uniform incorporation of niosomal vesicles within the Carbopol 934 gel matrix, which facilitates prolonged and consistent drug release through the membrane. The optimized formulation (F1) was selected based on experimental evaluation, specifically its higher entrapment efficiency and sustained drug-release profile, rather than on a desirability function or composite desirability score.

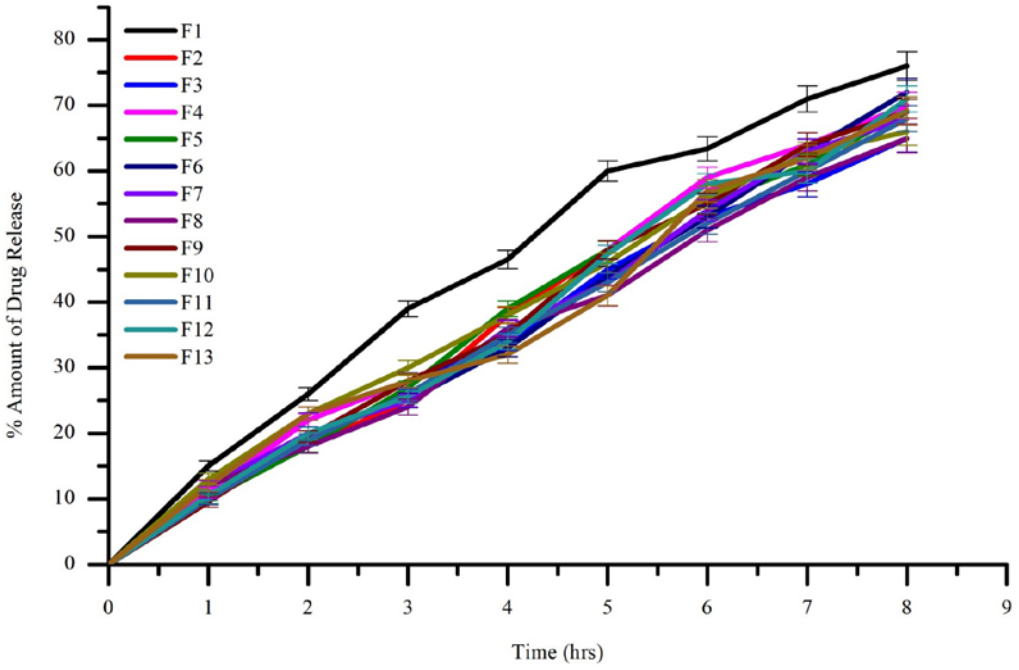

Figure 9: *In-Vitro* diffusion studies

Release Kinetics

The drug release mechanism was analysed using various kinetic models. In the Hixson-Crowell model, which accounts for drug release because of fluctuations in surface area of the carrier, best fits the release kinetics of the niosome system (R^2 = 0.9959). This suggests that drug release from the niosomes is through erosion or dissolution of the carrier.

Role of surfactant composition and charge in stability

The physicochemical characteristics of niosomes are mainly influenced by the surfactant's alkyl chain length and the cholesterol ratio. Short-chain surfactants such as Span 20 promote higher bilayer curvature and more compact packing, yielding smaller, more uniform vesicles, whereas longer-chain surfactants such as Span 80 produce larger, less stable structures.

Cholesterol enhances bilayer rigidity and entrapment efficiency by reducing membrane permeability; however, excess cholesterol may over-stiffen the bilayer and hinder drug release. The optimized Span 20–cholesterol ratio in this study produced nanosized vesicles (181 nm) with high EE (91%) and sustained release consistent with the Hixson–Crowell model. The measured zeta potential (–27 mV) indicates sufficient electrostatic and steric stabilization, supporting colloidal stability during storage.

Evaluation of Physical Appearance

As shown in Table 7, the prepared niosomal gel possessed desirable physical attributes, including acceptable colour, odour, and consistency.

Table 7: Physical Appearance of Niosomal gel

Characterization	Results
Colour	White
Odour	Odourless
Consistency	Smooth and Homogenous consistency and free from lump and air bubbles

pH Measurement

The mean pH of the niosomal gel is 5.5 ± 0.1, within the natural pH range of human skin. This indicates that the gel is well-suited for external application and is unlikely to irritate the skin or disrupt the skin's natural acid mantle. A standard deviation of 0.1 indicates that the pH values are uniform across the three batches (Table 8). It is important to maintain an optimal pH to ensure the stability and efficacy of gel preparations.

Table 8: pH of Niosome Formulation

pH readings	PH values ± S. D
Reading 1	5.5 ± 0.1
Reading 2	5.6 ± 0.1
Reading 3	5.4 ± 0.1

Viscosity

Niosomal gel viscosity was 3250 cP, which reflects its flow and consistency characteristics. A reading of 3250cP for the viscosity indicates that the niosomal gel is within a suitable range for application in topical formulations. This viscosity enables the gel to possess a correct consistency for facilitating the easy application and adhesion onto the skin with controlled release of the encapsulated active agents [26]. These rheological and physicochemical properties not only support enhanced dermal adherence and controlled drug diffusion but also indicate the formulation's practical suitability for clinical use and patient comfort.

Spreadability

The spreadability of the niosomal gel was tested and evaluated to assess its performance (Table 9). As the results indicate, the spreadability of the niosomal gel increases with increasing applied weight.

Table 9: Spreadability of the niosomal gel

Weight (g)	Initial Diameter (cm)	Final Diameter (cm)	Spreadability (g·cm/s)
20 g	2.0 ± 0.0	3.5 ± 0.1	0.10 ± 0.01
50 g	2.0 ± 0.0	5.0 ± 0.2	0.50 ± 0.05
100 g	2.0 ± 0.0	7.0 ± 0.3	1.67 ± 0.10

All determinations were performed in triplicate, and data are expressed as mean ± standard deviation (SD). Statistical comparisons were made using one-way ANOVA, and differences were considered significant at $p < 0.05$.

Comparative evaluation with recent niosomal/trans-ethosomal gel studies indicates that vesicular carriers consistently outperform conventional gels in stability, skin retention, and release control. For example, optimized niosomal gels have been reported to improve entrapment, sustain release, and enhance ex vivo skin deposition compared with non-vesicular gels. Our formulation (181 nm, EE 91%, zeta potential −27 mV, pH 5.5, viscosity 3250 cP; 75.0 ± 2.2% release at 8 h) shows comparable performance in nanosizing, entrapment, and diffusion control to recent reports on optimized niosomal systems. These findings corroborate published evidence that statistically optimized vesicular gels provide reduced burst release, prolonged release windows, and improved colloidal stability relative to conventional topical gels, supporting the translational promise of the present formulation [27,28].

CONCLUSION

The present work has demonstrated that the design of a miconazole nitrate niosomal gel, optimized using Box–Behnken statistical modelling, can effectively overcome the inherent challenges of poor solubility and limited dermal permeability associated with the drug. The study established that surfactant concentration played a pivotal role in governing vesicle size, homogeneity, and stability, while hydration volume and sonication parameters contributed to fine-tuning the physicochemical characteristics. The optimized formulation

achieved nanoscale vesicle size with narrow distribution, a highly stable zeta potential, and excellent entrapment efficiency, thereby confirming its robustness as a delivery system.

Comprehensive characterization reinforced the integrity of the formulation. FTIR analysis ruled out any significant drug-excipient incompatibilities, DSC profiles indicated favourable thermal behaviour, and SEM images confirmed uniform vesicular morphology. *In-vitro* diffusion studies provided further insight into the release mechanism, with the Hixson–Crowell kinetic model suggesting an erosion-controlled process. The incorporation of optimized vesicles into a Carbopol-based gel yielded a formulation with ideal pH, viscosity, and spreadability, making it pharmaceutically elegant and dermally acceptable. These results highlight that the developed niosomal gel represents a promising alternative to conventional topical antifungal preparations. By enhancing drug solubility, prolonging release, and potentially improving therapeutic efficacy, this system addresses important limitations of current formulations. However, the present investigation was limited to in-vitro characterization and diffusion analysis. Further *ex vivo and in vivo* skin permeation studies are warranted to validate dermal deposition and therapeutic performance. Additionally, microbial inhibition assays should be conducted to confirm the antifungal enhancement suggested by the formulation's release behavior. Future work will focus on evaluating the formulation's stability, shelf-life, and clinical applicability to establish its translational potential for commercial development.

FINANCIAL ASSISTANCE
NIL

CONFLICT OF INTEREST
The authors declare no conflict of interest.

AUTHOR CONTRIBUTION
Akash Mummoorthy contributed to the study's conceptualization, methodology development, and preparation of the original manuscript draft. Anbarasan Balu was responsible for conceptualization, investigation, and overall supervision of the work. Aravind Karthikeyan handled validation and data collection support and contributed to the review, editing, and interpretation of the results. Data curation was carried out by Aravind Karthikeyan, Kaviya Suresh, and Akash Rajendran, who also contributed to visualization. Akash Mummoorthy and Aravind Karthikeyan provided essential resources required for the study. All authors have made substantial, direct, and intellectual contributions to the work and have approved the final version for publication.

REFERENCES
[1] Maciel AAM, Cunha FA, Freire TM, de Menezes FL, Fechine LMUD, Rocha JS, de Cássia Carvalho Barbosa R, Martins RT, da Conceição dos Santos Oliveira Cunha M, Santos-Oliveira R, Queiroz MVO, Fechine PBA. Development and evaluation of an anti-candida cream based on silver nanoparticles. *3 Biotech*, **13**, 180 (2023) https://doi.org/10.1007/s13205-023-03776-9

[2] Tan Y, Shao Y, Li T, Hu X, Wang X, Wan Z, Yin F, Li R, Wang R. The effect of topical ketoconazole and topical miconazole nitrate in modulating the skin microbiome and mycobiome of patients with tinea pedis. *Mycoses*, **68**, e70116 (2025) https://doi.org/10.1111/myc.70116

[3] Regidor PA, Thamkhantho M, Chayachinda C, Palacios S. Miconazole for the treatment of vulvovaginal candidiasis: in vitro, in vivo and clinical results. Review of the literature. *J Obstet Gynaecol*, **43**, 1–8 (2023) https://doi.org/10.1080/01443615.2023.2195001

[4] Abdel-Rashid RS, Helal DA, Alaa-Eldin AA, Abdel-Monem R. Polymeric versus lipid nanocapsules for miconazole nitrate enhanced topical delivery: in vitro and ex vivo evaluation. *Drug Deliv*, **29**, 1–14 (2022) https://doi.org/10.1080/10717544.2022.2026535

[5] Kandekar U, Lotake S, Pandit A, Sayare A, Ghode P. Optimization of invasomal gel of miconazole nitrate for the treatment of topical fungal infections. *J Drug Deliv Sci Technol*, **104**, 106450 (2025) https://doi.org/10.1016/j.jddst.2024.106450

[6] Soutome S, Otsuru M, Kawashita Y, Yoshimatsu M, Funahara M, Murata M, Ukai T, Umeda M, Saito T. A preliminary study of suppression of candida infection by miconazole mucoadhesive tablets in oral or oropharyngeal cancer patients undergoing radiotherapy. *Sci Rep*, **12**, 10123 (2022) https://doi.org/10.1038/s41598-022-14269-9

[7] Ordaya EE, Clement J, Vergidis P. The role of novel antifungals in the management of candidiasis: a clinical perspective. *Mycopathologia*, **188**, 1–15 (2023) https://doi.org/10.1007/s11046-023-00759-5

[8] Li G. Miconazole in pharmacy: the safety profile in antifungal therapy. *Adv Pharmacoepidemiol Drug Saf*, **12**, 1000320 (2023) https://doi.org/10.35248/2167-1052.23.12.320

[9] Ding L, Yin L, Wang L, Sun Y, Liu X, Li X. Effectiveness of redcore lotion in patients with vulvovaginal candidiasis: a systematic review and meta-analysis. *J Tradit Chin Med*, **63(4)**, 1–10 (2022) https://doi.org/10.19852/j.cnki.jtcm.2022.04.001

[10] Jawale JK, Kashikar VS. An overview on nano niosomes: as an optimistic drug delivery system in targeted drug delivery. *J*

Pharm Res Int, **34**, 1–15 (2022) https://doi.org/10.9734/jpri/2022/v34i34a36142

[11] Antonara L, Triantafyllopoulou E, Chountoulesi M, Pippa N, Lagopati N, Dallas PP, Rekkas DM, Gazouli M. Recent advances in niosome-based transdermal drug delivery systems. *Curr Opin Biomed Eng*, **35**, 100603 (2025) https://doi.org/10.1016/j.cobme.2025.100603

[12] Witika BA, Bassey KE, Demana PH, Siwe-Noundou X, Poka MS. Current advances in specialised niosomal drug delivery: manufacture, characterization and drug delivery applications. *Int J Mol Sci*, **23**, 9668 (2022) https://doi.org/10.3390/ijms23179668

[13] Kumavat S, Sharma PK, Koka SS, Sharma R, Gupta A, Darwhekar GN. A review on niosomes: potential vesicular drug delivery system. *J Drug Deliv Ther*, **11**, 1–10 (2021) https://doi.org/10.22270/jddt.v11i5.5046

[14] Liga S, Paul C, Moacă EA, Péter F. Niosomes: composition, formulation techniques, and recent progress as delivery systems in cancer therapy. *Pharmaceutics*, **16**, 223 (2024) https://doi.org/10.3390/pharmaceutics16020223

[15] Ghumman SA, Ijaz A, Noreen S, Aslam A, Kausar R, Irfan A, Latif S, Shazly GA, Shah PA, Rana M, Aslam A, Altaf M, Kotwica-Mojzych K, Bin Jardan YA. Formulation and characterization of curcumin niosomes: antioxidant and cytotoxicity studies. *Pharmaceuticals*, **16**, 1406 (2023) https://doi.org/10.3390/ph16101406

[16] Tareen FK, Shah KU, Ahmad N, Asim-ur-Rehman N, Shah SU, Ullah N. Proniosomes as a carrier system for transdermal delivery of clozapine. *Drug Dev Ind Pharm*, **46**, 1–11 (2020) https://doi.org/10.1080/03639045.2020.1764020

[17] Bashkeran T, Kamaruddin AH, Ngo TX, Suda K, Umakoshi H, Watanabe N, Nadzir MM. Niosomes in cancer treatment: a focus on curcumin encapsulation. *Heliyon*, **9**, e18710 (2023) https://doi.org/10.1016/j.heliyon.2023.e18710

[18] Agarwal S. Formulation and in vitro evaluation of fluconazole niosomal gel for topical drug delivery. *J Pharm Negat Results*, **14**, 3963–75 (2023) https://doi.org/10.47750/pnr.2022.13.s08.498

[19] Kaur P, Rani R, Singh AP, Singh AP. An overview of niosomes. *J Drug Deliv Ther*, **14**, 1–12 (2024) https://doi.org/10.22270/jddt.v14i3.6450

[20] Chatur VM, Dhole SN, Kulkarni NS, Rudrapal M. Development and characterization of antifungal niosomal gel of luliconazole: in vitro and ex vivo approaches. *Chem Phys Impact*, **10**, 100801 (2025) https://doi.org/10.1016/j.chphi.2024.100801

[21] Purohit SJ, Tharmavaram M, Rawtani D, Prajapati P, Pandya H, Dey A. Niosomes as cutting edge nanocarrier for controlled and targeted delivery of essential oils and biomolecules. *J Drug Deliv Sci Technol*, **73**, 103438 (2022) https://doi.org/10.1016/j.jddst.2022.103438

[22] Hemmati J, Chegini Z, Arabestani MR. Niosomal-based drug delivery platforms: a promising therapeutic approach to fight Staphylococcus aureus drug resistance. *Biomed Res Int*, **2023**, 5298565 (2023) https://doi.org/10.1155/2023/5298565

[23] Tulbah AS, Elkomy MH, Zaki RM, Eid HM, Eissa EM, Ali AA, Yassin HA, Aldosari BN, Naguib IA, Hassan AH. Novel nasal niosomes loaded with lacosamide and coated with chitosan: a possible pathway to target the brain to control partial-onset seizures. *Int J Pharm X*, **6**, 100206 (2023) https://doi.org/10.1016/j.ijpx.2023.100206

[24] Shah P, Goodyear B, Haq A, Puri V, Michniak-Kohn B. Evaluations of quality by design (QbD) elements impact for developing niosomes as a promising topical drug delivery platform. *Pharmaceutics*, **12**, 246 (2020) https://doi.org/10.3390/pharmaceutics12030246

[25] Mishra S, Gupta RA. Formulation and evaluation of niosomal gel of antifungal luliconazole. *J Drug Deliv Ther*, **12**, 1–10 (2022) https://doi.org/10.22270/jddt.v12i6-s.5705

[26] Shah N, Prajapati R, Gohil D, Aundhia C, Sadhu P, Kardani S. Luliconazole loaded niosomal topical gel: factorial design, in vitro characterization and antifungal study. *Indian J Pharm Educ Res*, **57**, 1–10 (2023) https://doi.org/10.5530/ijper.57.3s.60

[27] Aldawsari MF, Khafagy ES, Moglad EH, Selim Abu Lila A. Formulation optimization, in vitro and in vivo evaluation of niosomal nanocarriers for enhanced topical delivery of cetirizine. *Saudi Pharm J*, **31**, 1–12 (2023) https://doi.org/10.1016/j.jsps.2023.101734

[28] Alsaidan OA, Zafar A, Al-Ruwaili RH, Yasir M, Alzarea SI, Alsaidan AA, Singh L, Khalid M. Niosomes gel of apigenin to improve the topical delivery: development, optimization, ex vivo permeation, antioxidant study, and in vivo evaluation. *Artif Cells Nanomed Biotechnol*, **51**, 1–15 (2023) https://doi.org/10.1080/21691401.2023.2274526